

EFFECT OF CaCO_3 AND LIME GLASS USING TO PORE STRUCTURE FORMING ON A CERAMIC GLASS BASED ON SCORIA BASALT ROCKS

PENGARUH PENGGUNAAN CaCO_3 DAN LIME GLASS DALAM PEMBENTUKAN STRUKTUR BERPORI PADA GLASS CERAMIC BERBASIS BATUAN BASALT SKORIA

DAVID C. BIRAWIDHA¹, YUSUP HENDRONURSITO¹, KUSNO ISNUGROHO¹, MUHAMMAD AMIN¹, ANTON S. HANDOKO^{1*}, SENTAUZA NURINGJATI², and SYAFRIADI²

¹ Research Unit for Mineral Technology – National Research and Innovation Agency

Jl. Ir. Sutami Km. 15 Tanjung Bintang, Lampung Selatan, Indonesia

² Departement of Physics, FMIPA, Universitas Lampung

Jl. Prof. Dr. Soemantri Brojonegoro No.1 Gedung Meneng,
Bandar Lampung 35145, Lampung, Indonesia

* Corresponding author's email: e_electrical@yahoo.com

ABSTRACT

Technological developments occur at this time cause the technology for making lightweight materials is also growing. The technology for making lightweight materials aims to reduce the total weight of the material without reducing its mechanical strength. Parameters that influence the manufacture of lightweight materials are the number of pores, material density, and physical resistance. One of the commonly used methods is mixing the ceramic glass with a foaming agent. In this study, the basalt rock from East Lampung, Indonesia and the lime glass were used as a ceramic glass material. Variations in its composition were carried out by mass comparison between the basalt and the lime glass, namely Sample A (100:0), Sample B (70:30), Sample C (50:50), and Sample D (30:70) with 50%wt. CaCO_3 added to each sample and heated up to 1200 °C. Cooling variations (annealed and normalized) are also applied to see the occurred phenomena. Based on the characterization results, the best sample is Sample B with normalized cooling and has a porosity value of 53.2% and a density value of 1.08 gr/cm³. Based on the SEM test results, the pores with a size of $\leq 0.5\mu\text{m}$ are 95%, and $\geq 0.5\mu\text{m}$ are 5% in which the crystals formed are pyroxene and calcite with the compositions of CaO and SiO_2 39.46% and 41.90% respectively.

Keywords: basalt, CaCO_3 , lime glass, foam agent, light material.

ABSTRAK

Perkembangan teknologi yang terjadi saat ini menyebabkan teknologi pembuatan material ringan juga semakin berkembang. Teknologi pembuatan material ringan tersebut bertujuan untuk mengurangi berat total tanpa mengurangi kekuatan mekanis suatu material. Parameter yang mempengaruhi pembuatan material ringan adalah jumlah pori, berat jenis material dan ketahanan fisik. Salah satu metode yang umum digunakan adalah mencampurkan glass ceramic dengan foaming agent. Pada penelitian ini digunakan batuan basalt dari Lampung Timur, Indonesia dan serbuk kaca (lime glass) sebagai material glass ceramic. Variasi komposisi dilakukan dengan perbandingan antara basalt dan lime glass yaitu sampel A (100:0), sampel B (70:30), sampel C (50:50), dan sampel D (30:70) yang ditambahkan 50 % berat CaCO_3 dan dilebur pada suhu 1200 °C. Variasi pendinginan (annealed dan normalizing) juga diterapkan untuk melihat fenomena yang terjadi. Berdasarkan hasil karakterisasi yang dilakukan, sampel terbaik terdapat pada sampel B dengan pendinginan normalizing yang mempunyai nilai porositas sebesar 53,2% dan untuk nilai densitas 1,08 g/cm³. Berdasarkan hasil uji SEM, pori-pori dengan ukuran $\leq 0,5\mu\text{m}$ sebanyak 95% dan ukuran $\geq 0,5\mu\text{m}$ sebanyak 5%. Kristal yang terbentuk pada kondisi tersebut adalah piroksen dan kalsit dengan komposisi CaO dan SiO_2 berturut-turut adalah 39,46% dan 41,90%.

Kata kunci: basalt, CaCO_3 , lime glass, foam agent, material ringan.

INTRODUCTION

Technology development lately affects the progress of lightweight material making that can reduce the total weight without reducing its mechanical strength. Lightweight material can make the work easier, cheaper, environmentally friendly, and have a greater effect on comfort, longevity, and application speed (Trinugroho and Murtono, 2015). The lightweight material is chosen not only because it can reduce the total weight material, but also because it can make it stronger and more efficient. This lightweight material was chosen as an alternative material (Purwasasmita and Roland, 2008).

There are many types of light material products, and the common ones found are mild steel (Tanto, Dewi and Budio, 2012), namely titanium which is used as an aircraft fuselage (Uhlmann *et al.*, 2015), and lightweight brick, which is a cellular (porous) concrete (Hunggurami, Bunganaen and Muskanan, 2014). Composite materials can also make strong lightweight, and corrosion-resistant materials (Banowati, Fauzan and Suprihanto, 2019).

Lightweight materials are built by two constituent parts: the solid and the cavity parts filled by gas or air phase. This cavity is the influence role of the foaming substance (foam producer). A foaming substance is a cavity-forming agent widely used in the light material manufacturing industry. The cavity; functions as an air wrapping medium that produces pores so that the material becomes light (Rajiman and Listari, 2019). The addition of foaming agent can cause the pores to be the material mechanically strong. These results depend on the composition and the used method (Kusharjanto, Dwiwanto and Atmawijaya, 2013).

In the classification of rocks and non-metallic minerals other than perlite, basalt has the potential to be used as a base material for manufacturing light-porous materials (Marangoni *et al.*, 2014). Basalt is a rock formed from frozen lava above the ground surface. The mineral is fine-grained black in color. Indonesia has abundant natural material wealth, but currently, the use of these materials has not been maximized (Suharto *et al.*, 2020). This rock is one of the potential mineral resources in Lampung province. The

minimum amount of its reserves is 336 million m³ (Rajiman and Aulia, 2019).

Previous research of manufacturing foam glass, the foam glass structures are generally prepared using a high-temperature process, usually using foaming agents (Bai *et al.*, 2014) such as aluminum (Yang *et al.*, 2020), MgAl₂O₄ (Deng *et al.*, 2016), and the most widely used is calcium carbonate (CaCO₃). CaCO₃ has abundant availability, around 2,160 billion tons, where the magnitude of this potential is accompanied by a large consumption of limestone (Chen *et al.*, 2012). In the formation of the foam structure using basalt scoria, Marangoni *et al.* (2014) studied the use of lime glass to generate bubbles for its foaming process. Carbonate element addition in lime glass can stimulate the bubbles forming at high temperatures but has less stable tendency in the formation of its foam structure (Dhir *et al.*, 2018).

In this study, scoria basalt rock was derived from Mataram Baru of East Lampung was mixed with the lime glass as a raw material for the ceramic glass, later on, it will be modified to be porous using the foaming agent CaCO₃ to increase the chance of foam formation. Scoria basalt itself have different characteristic compared to other basalt types. From a visual perspective, the basalt has a sponge morphology on its surface so it is easy to differentiate from other rocks (Birawidha *et al.*, 2020). Variations in composition and cooling were used to determine the optimal results of the porous structure formed in the ceramic glass sample.

METHODOLOGY

Equipment used in this research were: Nabertherm 1800 °C furnace, ball mill, 100 mesh sieve with ASTM Type E11 Nakatama Scientific, digital scale DENPO for porosity and density measurement using Archimedes method, Scanning Electron Microscope Energy Dispersive X-Ray (SEM-EDX) type Quatro Thermo scientific, X-ray Diffraction (XRD) PANalytical type E'xpertPro, and X-ray Fluorescence (XRF). The materials used in this research process include activated CaCO₃ from PT. Dwi Selo Giri Mas, Sidoarjo, lime glass made from used glass and basalt rock from Mataram Baru, East Lampung.

In this research, the process was divided into 4 stages; preparation, making sample for laboratory testings, physical testing (density and porosity), and characterization the samples by XRF, XRD, and SEM. In preparation stage, the basalt and the lime glass materials were ground using a ball mill. Then the basalt, lime glass, and CaCO₃ were filtered using a 100-mesh sieve so that the size was uniform above +100 mesh. Furthermore, the XRF analysis was carried out on all materials. After the preparation stage, the next stage was sample making, as shown in Table 1, which refers to the research of Marangoni *et al.* (2014) for the research procedure.

Table 1. Sample making

Material	Sample A (%)	Sample B (%)	Sample C (%)	Sample D (%)
Basalt	100	70	50	30
Lime glass	0	30	50	70

*All material variations are added with CaCO₃ of 50% wt.

The sample whose composition has been varied was then inserted and mixed into a mold with good heat resistance. Then the sample was burned at a temperature of 1200 °C for 90 minutes. After the burning process was finished, cooling was carried out. This study has two cooling variations: cooling inside the furnace (annealed) and outside the furnace (normalizing to room temperature). Then the samples were subjected to physical tests, such as density, and porosity tests, and later on, characterization sample tests using XRF, XRD, and SEM.

RESULTS AND DISCUSSION

Basalt from East Lampung has a dominant composition of SiO₂ and Al₂O₃ (Amin and Suharto, 2017). The results of the same analysis are shown in the scoria basalt rock in East Lampung used in this study (Table 2). SiO₂ exists not only in basalt but also in lime glass where the glass material is crystalline. Quartz rich in SiO₂ (Demirsöz *et al.*, 2022). As for activated CaCO₃ based on Table 2, CaO has a percentage of 88.91%, whereas the dominant compound for CaCO₃ has a value above 80% (Megawati, Alimuddin and Kadir, 2019). This condition becomes potential for foaming and facilitating the formation of the

porous structure in the scoria basalt rock because CaO is a valuable element to produce foam that can cause a foaming effect (Sutarno *et al.*, 2015). The results of XRF basalt, CaCO₃ (activated), and lime glass can be seen in Table 2.

Tabel 2. XRF analysis results from basalt, CaCO₃, and lime glass

Compound	Basalt (%wt)	CaCO ₃ Activated (%wt)	Lime glass (%wt)
MgO	4.56	10.43	2.3
Al ₂ O ₃	18.82	0.25	2.0
SiO ₂	48.41	-	73.8
CaO	9.76	88.91	16.8
Fe ₂ O ₃	12.59	0.22	3.4
Na ₂ O	3.35	-	-
K ₂ O	0.63	-	0.3
TiO ₂	1.32	-	0.2
MnO	0.19	-	0.1

Based on Table 3, the greater the basal composition, the greater the SiO₂ compound contained in the sample. Sample A has the highest SiO₂ compound content, which is 48.42% because basically, basalt itself contains SiO₂ compounds (Liu *et al.*, 2018). The addition of CaCO₃ material by 50% in each variation except Sample A functions as a gas bubble producer during the heating up to 1200 °C. The gas formation is influenced by the composition of CaCO₃ where it decomposes into CaO and CO. The highest CaO compound was detected in Sample B at 39.46% as shown in Table 3.

Table 3. XRF analysis results from the mixed sample (basalt, CaCO₃, and lime glass) after smelting

Compound	(A)	(B)	(C)	(D)
MgO	4.56	8.94	6.80	7.10
Al ₂ O ₃	18.82	5.73	5.31	3.59
SiO ₂	48.41	41.90	40.00	31.01
SO ₃	-	0.47	-	0.61
K ₂ O	0.63	0.21	0.31	0.35
CaO	9.76	39.46	36.14	38.27
TiO ₂	1.32	0.59	0.85	1.02
MnO	0.19	0.22	0.31	0.39
Fe ₂ O ₃	12.59	11.88	9.71	7.10

The decrease in the use of basalt also affects the amount of Fe₂O₃ compound content, which is also decreased. The highest Fe₂O₃ content of 12.59% was detected in Sample A

because the iron compounds in basalt are generally high enough even without a mixture of other ingredients as shown in Table 3. Sample A has the highest iron content (Davis and Cottrell, 2021). The content of alumina

compounds in the sample also changes when the basalt is varied materials as samples B, C, and D. It can be concluded that the higher the basalt concentration, the higher the alumina content, and vice versa.

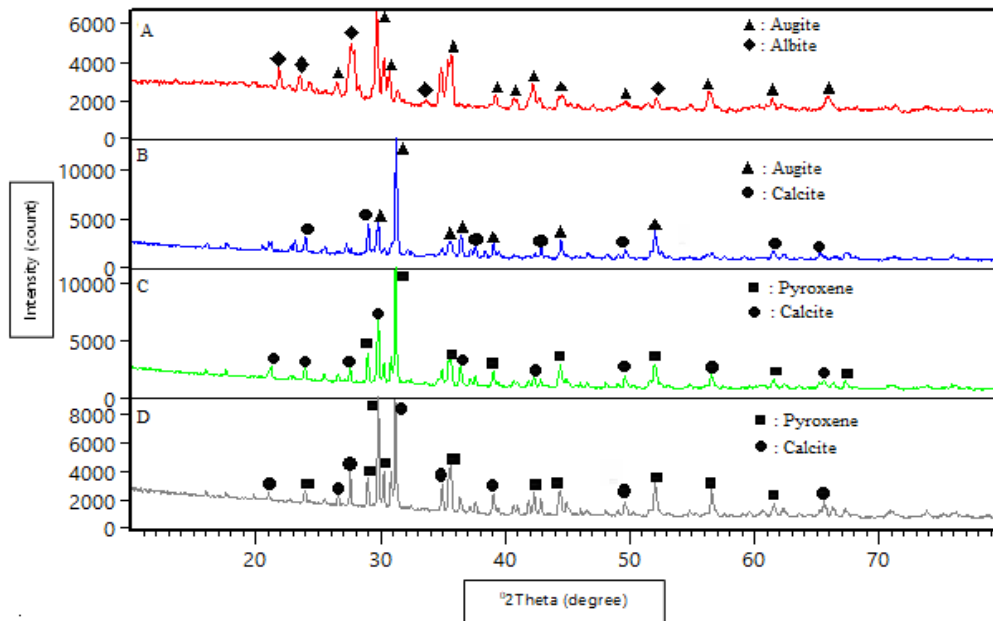


Figure 1. Diffractogram of XRD characterization results with annealed cooling

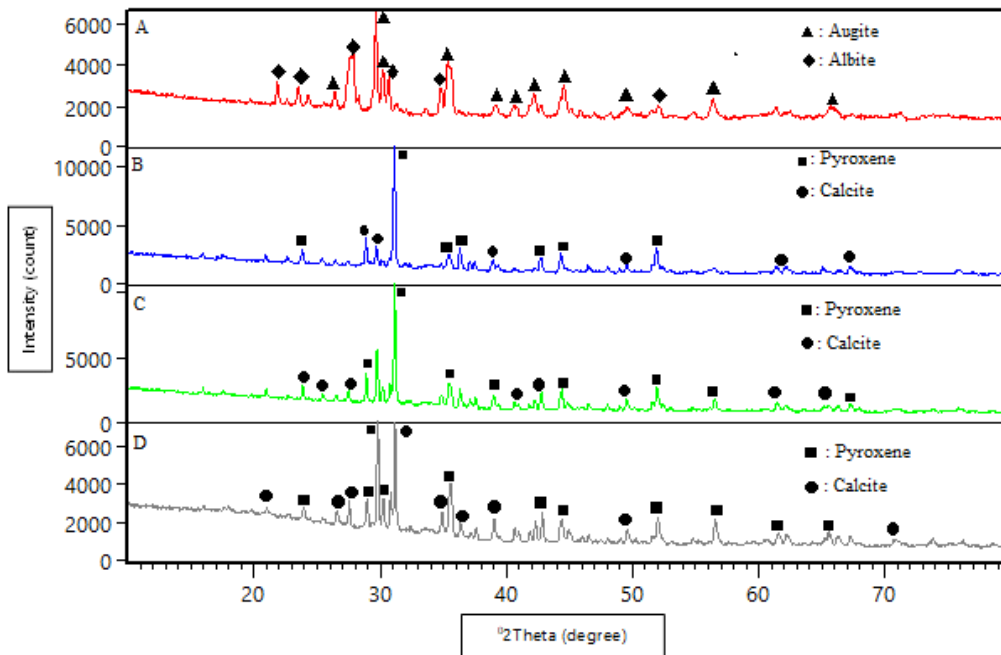


Figure 2. Diffractogram of sample XRD test results with normalizing cooling

Based on the XRD results in Figure 1, the phases detected differ among samples B, C, and D which have the same variety of material on annealed cooling. The crystal structure that occurred in Sample B (70% basalt) detected a phase dominated by a monoclinic structure with augite mineral group - $(\text{Ca},\text{Na})(\text{Mg},\text{Fe},\text{Al},\text{Ti})(\text{Si},\text{Al})_2\text{O}_6$ which is a pyroxene group with the highest intensity at 2θ is 31.2190, and the calcite (CaCO_3) phase with the highest intensity at 2θ is 28.9780. Meanwhile, samples C and D detected the pyroxene phase $((\text{XY}(\text{Si},\text{Al})_2\text{O}_6))$ with the highest intensity at 2θ is 29.9600 and calcite (CaCO_3) with the highest intensity at 2θ is 28.9780 which have in common with Demenev result (Demenev *et al.*, 2021). Sample B with the variation of basalt is more dominant than that

of the lime glass. It has affected the growth of augite due to the dominant Ca and Mg, as shown in table 3. Meanwhile, in Sample A with 100% basalt, the detected phases are augite and albite ($\text{NaAlSi}_3\text{O}_8$) which are produced by the element alumina as stated in Suharto's research (Suharto *et al.*, 2020).

The XRD characterization result of the sample with normalized cooling showed the different phases with the annealed cooling. Samples B, C, and D in normalized cooling exhibit the same phase, namely the pyroxene phase $((\text{XY}(\text{Si},\text{Al})_2\text{O}_6))$. This was because that during the burning process at 1200 °C with faster cooling, the elements Ca and Mg are decreasing. These elements affect the formation of the augite phase (Guo *et al.*, 2020).

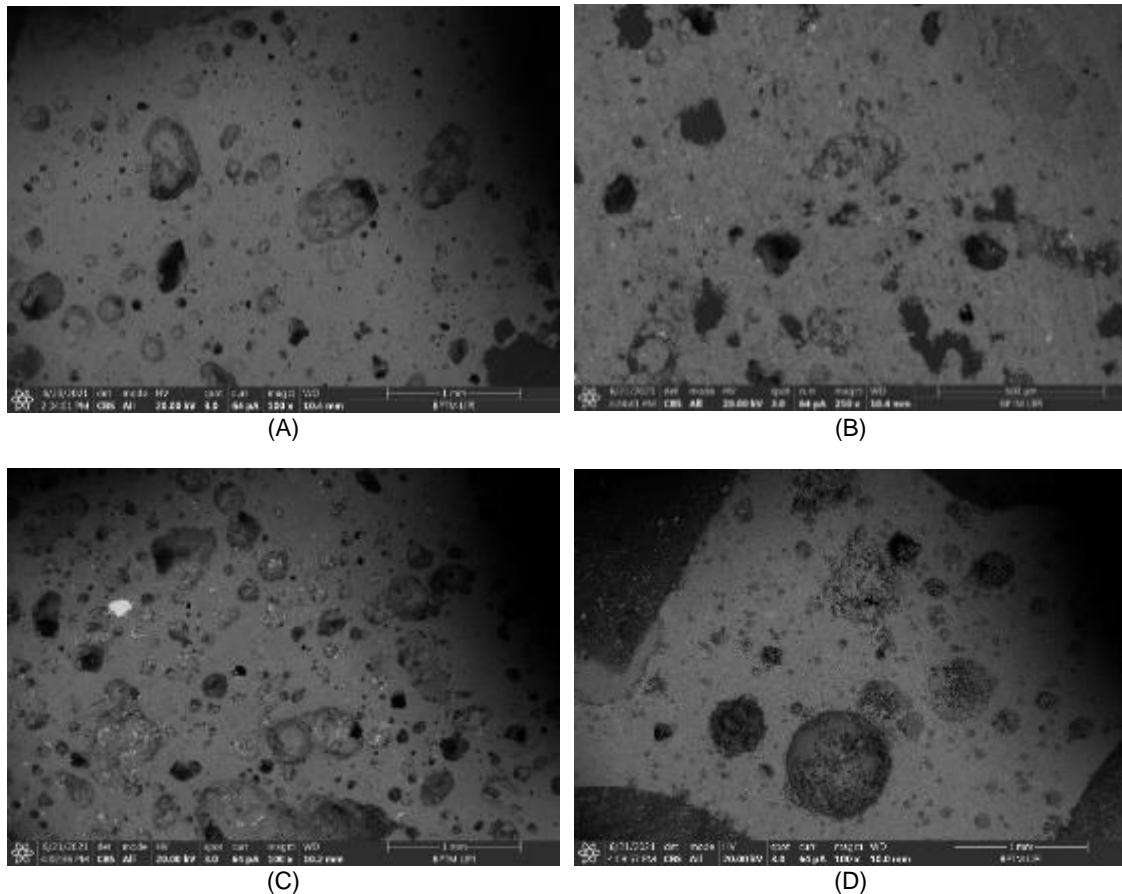


Figure 3. Results of SEM images with SE mode for annealed variation samples.

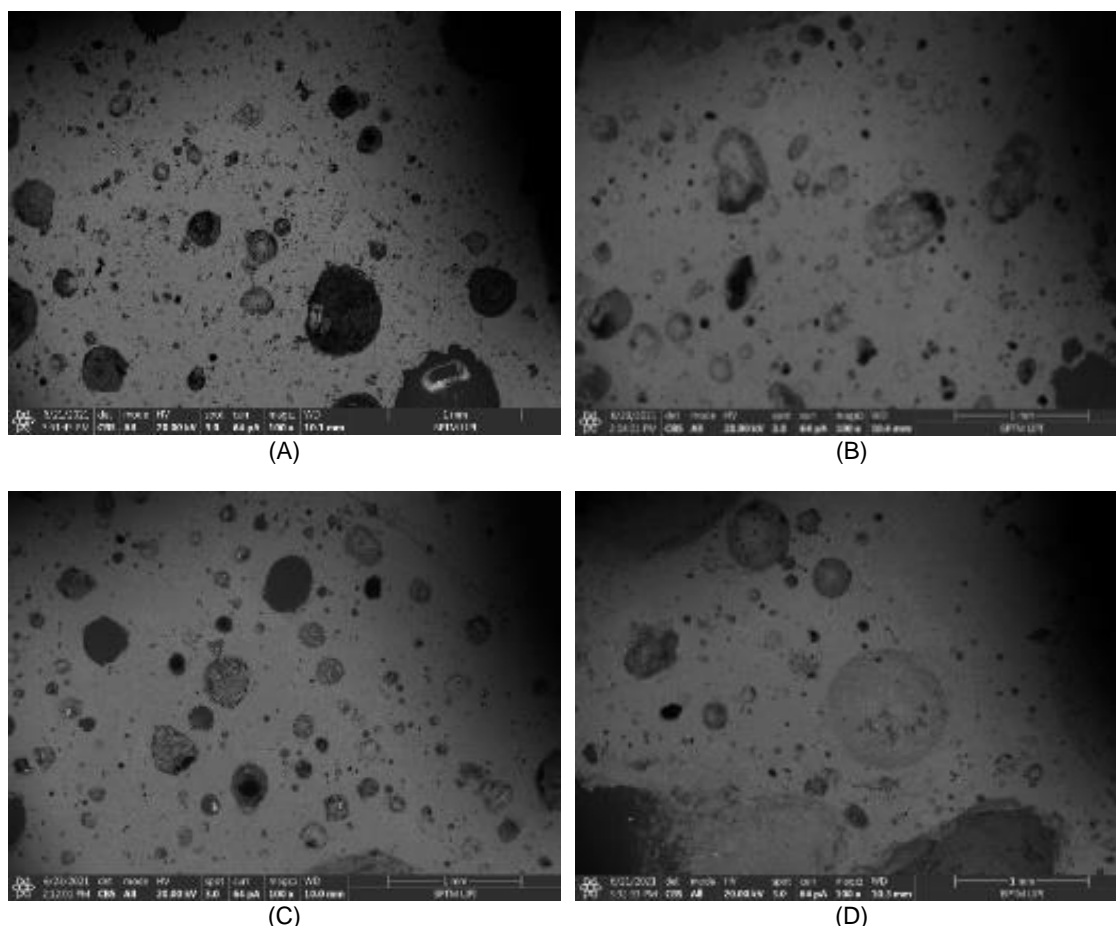


Figure 4. Results of SEM images with SE mode for normalizing variation samples.

It can be seen in Figure 3 that the annealed cooling sample shows different morphological forms of pores based on their size at 100x magnification. In Sample A with 100% basalt material, the pores that is formed with a size of $\leq 0.5\mu\text{m}$ are 85% and $\geq 0.5\mu\text{m}$ are 15%. In Sample B all the formed pores have a size of $\leq 0.5\mu\text{m}$, in Sample C, the formed pores with a size of $\leq 0.5\mu\text{m}$ are 75% and a size of $\geq 0.5\mu\text{m}$ are 25%. In Sample D the pores is formed with a size of $\leq 0.5\mu\text{m}$ as much as 60% and a size of $\geq 0.5\mu\text{m}$ as much as 40%. Although the annealed cooling Sample A has a relatively large percentage of small pores of 85% compared to Sample B in terms of the toughness of the material in distributing the load, the large number of small pores is more advantageous (Zahasky *et al.*, 2018).

It can be seen in Figure 4 that the samples with normalizing cooling showed different morphological shapes of pores based on their

size at 100x magnification. In Sample A with 100% basalt material, the pores are formed with a size of $\leq 0.5\mu\text{m}$ as much as 80% and a size of $\geq 0.5\mu\text{m}$ as much as 20%. In Sample B, the pores formed with a size of $\leq 0.5\mu\text{m}$ as much as 95% and a size of $\geq 0.5\mu\text{m}$ as much as 5%. In Sample C, the pores formed with a size of $\leq 0.5\mu\text{m}$ are 90% and a size of $\geq 0.5\mu\text{m}$ as much as 10%, while in Sample D the pores formed with a size of $\leq 0.5\mu\text{m}$ as much as 80% and a size of $\geq 0.5\mu\text{m}$ as much as 20%. In the sample with normalizing cooling process compared to other ceramic glass samples, Sample B has a better balance of pore composition with 95% pores with a size of $\leq 0.5\mu\text{m}$, in terms of toughness compared to other samples, the potential for uniformly dispersed loads is greater.

Based on Figure 5, the optimal variation occurs in Sample B, with annealed cooling having the highest porosity of 53.2%. Unlike when cooled slowly, at normalizing the

porosity formed is smaller by 27%. Percentage porosity calculation is based on the Archimedes method, using reference calculations SNI 03-6433-2000 and ASTM D-C 642-97 for density and porosity calculation. Based on SEM observations in Figures 3 and 4, although the percentage of pores with a diameter less than 0.5 μm more occurred in the annealed cooling sample, the overall quantity number of pores in the ceramic glass body with normalizing cooling was more formed.

Based on Figure 6, Sample B has the lowest density value of 1.08 g/cm³ with normalizing cooling which is in line with the porosity value, and inversely proportional to the density value (Sriyani and Partono, 2020). Overall the less use of basalt when mixed with lime glass, the percentage of porosity will decrease and the density will increase.

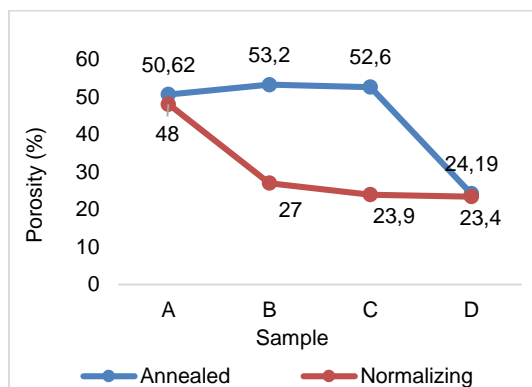


Figure 5. Porosity test results

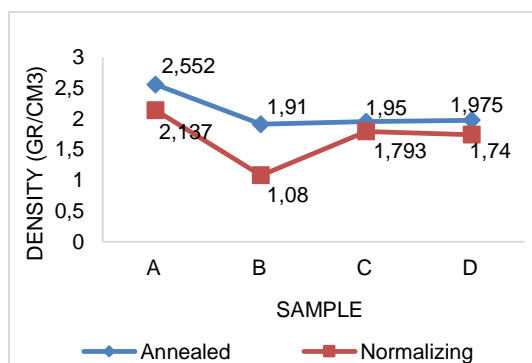


Figure 6. Density test results

CONCLUSIONS

In this study, with 50%wt CaCO₃ added to each sample, the optimal porous ceramic glass was made using 70% basalt and 30% lime glass (Sample B) which had silica and CaO content of 41.90% and 39.46%, respectively. Crystallization formed is pyroxene and calcite. In the formation of porous ceramics glass based on basalt and lime glass, the less the use of basalt, the porosity formed on average will decrease inversely with the increasing density.

ACKNOWLEDGMENTS

The authors acknowledge the facilities, scientific and technical support from Advanced Characterization Laboratories Lampung, Indonesian Institute of Sciences through E- Layanan Sains of Indonesian Institute of Sciences. Contributors statement: in this paper, David and Anton are the main contributors, and the rest are member contributors.

REFERENCES

- Amin, M. and Suharto (2017) 'Pembuatan semen geopolimer ramah lingkungan berbahan baku mineral basal guna menuju Lampung sejahtera', *Inovasi Pembangunan - Jurnal Kelitbangan*, 5(1), pp. 30–45.
- Bai, J., Yang, X., Xu, S., Jing, W. and Yang, J. (2014) 'Preparation of foam glass from waste glass and fly ash', *Materials Letters*, 136, pp. 52–54. doi: 10.1016/j.matlet.2014.07.028.
- Banowati, L., Fauzan, A. F. and Suprihanto, D. (2019) 'Analisis perbandingan kekuatan tarik komposit hybrid serat daun nanas – e-glass / epoxy bakalite EPR 174 dan hybrid serat daun nanas – e-glass / vinyl ester repxoy R 802', *INDEPT*, 8(3), pp. 69–76.
- Birawidha, D. C., Isnugroho, K., Hendronursito, Y., Amin, M. and Al Muttaqii, M. (2020) 'The x-ray diffraction (XRD) analysis of basalt from Mataram Baru via slow and rapid cooling process', *MULTITEK INDONESIA*, 13(2), pp. 6–14. doi: 10.24269/mtkind.v13i2.1945.

- Chen, B., Wang, K., Chen, X. and Lu, A. (2012) 'Study of foam glass with high content of fly ash using calcium carbonate as foaming agent', *Materials Letters*, 79, pp. 263–265.
doi: 10.1016/j.matlet.2012.04.052.
- Davis, F. A. and Cottrell, E. (2021) 'Partitioning of Fe₂O₃ in peridotite partial melting experiments over a range of oxygen fugacities elucidates ferric iron systematics in mid-ocean ridge basalts and ferric iron content of the upper mantle', *Contributions to Mineralogy and Petrology*, 176(9), p. 67.
doi: 10.1007/s00410-021-01823-3.
- Demenev, A. D., Khmurchik, V. T., Maksimovich, N. G., Demeneva, E. P. and Sedinin, A. M. (2021) 'Improvement of sand properties using biotechnological precipitation of calcite cement (CaCO₃)', *Environmental Earth Sciences*, 80(17), p. 580. doi: 10.1007/s12665-021-09818-w.
- Demirsöz, R., Korkmaz, M. E., Gupta, M. K., Collado, A. G. and Krolczyk, G. M. (2022) 'Erosion characteristics on surface texture of additively manufactured AlSi10Mg alloy in SiO₂ quartz added slurry environment', *Rapid Prototyping Journal*, 28(5), pp. 916–932. doi: 10.1108/RPJ-10-2021-0283.
- Deng, X., Wang, J., Liu, J., Zhang, H., Han, L. and Zhang, S. (2016) 'Low cost foam-gelcasting preparation and characterization of porous magnesium aluminate spinel (MgAl₂O₄) ceramics', *Ceramics International*, 42(16), pp. 18215–18222.
doi: 10.1016/j.ceramint.2016.08.145.
- Dhir, R. K., Brito, J. de, Ghataora, G. S. and Lye, C. Q. (2018) 'Use of glass cullet in ceramics and other applications', in *Sustainable Construction Materials*. Elsevier, pp. 327–387.
doi: 10.1016/B978-0-08-100984-0.00009-6.
- Guo, Z., Li, Y., Liu, S., Xu, H., Xie, Z., Li, S., Li, X., Lin, Y., Coulson, I. M. and Zhang, M. (2020) 'Discovery of nanophase iron particles and high pressure clinoenstatite in a heavily shocked ordinary chondrite: Implications for the decomposition of pyroxene', *Geochimica et Cosmochimica Acta*, 272, pp. 276–286.
doi: 10.1016/j.gca.2019.10.036.
- Hunggurami, E., Bunganaen, W. and Muskanan, R. Y. (2014) 'Studi eksperimental kuat tekan dan serapan air bata ringan cellular lightweight concrete dengan tanah putih sebagai agregat', *Jurnal Teknik Sipil*, 3(2), pp. 125–136.
- Kusharjanto, K., Dwiwanto, S. A. and Atmawijaya, W. (2013) 'Proses pembuatan aluminium foam berbahan baku skrap paduan AL-7075 dengan menggunakan CaCO₃ sebagai foaming agent', *Jurnal Riset Industri*, 7(2), pp. 159–172.
- Liu, J., Yang, J., Chen, M., Lei, L. and Wu, Z. (2018) 'Effect of SiO₂, Al₂O₃ on heat resistance of basalt fiber', *Thermochimica Acta*, 660, pp. 56–60.
doi: 10.1016/j.tca.2017.12.023.
- Marangoni, M., Secco, M., Parisatto, M., Artioli, G., Bernardo, E., Colombo, P., Altasi, H., Binmajed, M. and Binhussain, M. (2014) 'Cellular glass-ceramics from a self foaming mixture of glass and basalt scoria', *Journal of Non-Crystalline Solids*, 403, pp. 38–46.
doi: 10.1016/j.jnoncrysol.2014.06.016.
- Megawati, Alimuddin and Kadir, L. A. (2019) 'Komposisi kimia batu kapur alam dari industri kapur Kabupaten Kolaka Sulawesi Tenggara', *Jurnal Matematika, Sains, dan Pembelajarannya*, 5(2), pp. 104–108.
- Purwasasmita, B. S. and Roland, P. H. (2008) 'Karakterisasi dan fabrikasi material berpori untuk aplikasi pelet apung (floating feed)', *Bionatura*, 10(1), pp. 13–28.
- Rajiman and Aulia, I. (2019) 'Pengaruh penambahan serbuk batu basalt pada komposisi campuran beton menggunakan ordinary portland cement (OPC) ditinjau dari kuat tekan beton', *TAPAK (Teknologi Aplikasi Konstruksi)*, 9(1), pp. 9–17.
- Rajiman and Listari, V. (2019) 'Analisis variasi suhu pemanasan serbuk batu basalt sebagai bahan pengisi ordinary portland cement terhadap kuat tekan beton', *JRSDD*, 7(4), pp. 515–523.
- Sriyani, M. and Partono, P. (2020) *Studi pengecoran aluminium dengan metode centrifugal casting dengan variasi kemiringan cetakan 0°, 15°, 30° terhadap komposisi kimia, density, porositas dan struktur mikro*. Universitas Muhammadiyah Surakarta.
- Suharto, S., Amin, M., Al Muttaqii, M., Syafriadi, S. and Nurwanti, K. (2020) 'Pengaruh penggunaan batu basalt Lampung dan batubara dalam bahan baku terhadap karakteristik klinker', *Jurnal Teknologi Bahan dan Barang Teknik*, 10(1), pp. 49–57. doi: 10.37209/jtbbt.v10i1.167.

- Sutarno, Soepriyanto, S., Korda, A. A. and Dirgantara, T. (2015) 'Pengaruh kalsia alumina ($\text{CaO} \cdot \text{Al}_2\text{O}_3$) pada busa aluminium AL-7000 dengan agen pembusa kalsium karbonat (CaCO_3)', in *Prosiding Simposium Nasional Inovasi dan Pembelajaran Sains 2015 (SNIPS 2015)*. Bandung: Institut Teknologi Bandung, pp. 149–152.
- Tanto, D., Dewi, S. M. and Budio, S. P. (2012) 'Faktor-faktor yang mempengaruhi produktivitas pekerja pada pengerjaan atap baja ringan di perumahan Green Hills Malang', *Rekayasa Sipil*, 6(1), pp. 69–82.
- Trinugroho, S. and Murtono, A. (2015) 'Pemanfaatan foam agent dan material lokal dalam pembuatan bata ringan', in *Seminar Nasional Teknik Sipil V*. Surakarta: Universitas Muhammadiyah Surakarta, p. S-(49-58).
- Uhlmann, E., Kersting, R., Klein, T. B., Cruz, M. F. and Borille, A. V. (2015) 'Additive Manufacturing of Titanium Alloy for Aircraft Components', *Procedia CIRP*, 35, pp. 55–60. doi: 10.1016/j.procir.2015.08.061.
- Yang, D., Zhang, Z., Chen, X., Han, X., Xu, T., Li, X., Ding, J., Liu, H., Xia, X., Gao, Y., Wang, Y. and Sun, Y. (2020) 'Quasi-static compression deformation and energy absorption characteristics of basalt fiber-containing closed-cell aluminum foam', *Metals*, 10(7), p. 921. doi: 10.3390/met10070921.
- Zahasky, C., Thomas, D., Matter, J., Maher, K. and Benson, S. M. (2018) 'Multimodal imaging and stochastic percolation simulation for improved quantification of effective porosity and surface area in vesicular basalt', *Advances in Water Resources*, 121, pp. 235–244. doi: 10.1016/j.advwatres.2018.08.009.

